The optical properties of Tm^{3+} doped $Na_5Lu_9F_{32}$ single crystal*

SHENG Qi-guo (盛启国)[1], **XIA Hai-ping** (夏海平)[1]**, **TANG Qing-yang** (汤庆阳)[1], **HE Shi-nan** (何仕楠)[1], **ZHANG Jian-li** (章践立)[1], **and CHEN Bao-jiu** (陈宝玖)[2]

1. Key Laboratory of Photo-electronic Materials, Ningbo University, Ningbo 315211, China

2. Department of Physics, Dalian Maritime University, Dalian 116026, China

(Received 12 February 2017)

Tm^{3+} doped $Na_5Lu_9F_{32}$ single crystal with high optical quality was grown by an improved Bridgman method. The Judd-Ofelt intensity parameters Ω_t (t=2, 4, 6) were calculated according to the measured absorption spectra and physical-chemical properties of the obtained $Na_5Lu_9F_{32}$ single crystal. The stimulated emission cross-section of the $^3F_4 \rightarrow {}^3H_6$ transition (~1.8 μm) is 0.35×10^{-20} cm^2 for Tm^{3+} doped $Na_5Lu_9F_{32}$ single crystal. The emission spectra under the excitation of 790 nm laser diode (LD) and fluorescence lifetime at 1.8 μm were measured to reveal the fluorescence properties of Tm^{3+} doped $Na_5Lu_9F_{32}$ single crystal. The research results show that the Tm^{3+} doped $Na_5Lu_9F_{32}$ single crystal has larger stimulated emission cross-section compared with other crystals. All these spectral properties suggest that this kind of Tm^{3+}doped $Na_5Lu_9F_{32}$ crystal with high physical-chemical stability and high-efficiency emission at 1.8 μm may be used as potential laser materials for optical devices.

Document code: A **Article ID:** 1673-1905(2017)03-0201-5

DOI 10.1007/s11801-017-7025-6

Recently, much attention has focused on the Tm^{3+} doped single crystals because of their potential application in mid-infrared laser[1,2]. It is known that the transition of Tm^{3+} ($^3F_4 \rightarrow {}^3H_6$) can generate 1.8 μm laser radiation, and the cross relaxation energy transfer process ($^3H_6+{}^3H_4 \rightarrow {}^3F_4+{}^3F_4$) between Tm^{3+} ions has been demonstrated to increase the quantum efficiency of Tm^{3+} reaching about 200%[3,4]. Therefore, the Tm^{3+} doped laser crystals working at 1.8 μm are of wide tunability and high efficiency, as well as the advantage of direct diode pumping at ~800 nm[5].

Recently, Tm^{3+} doped $LiYF_4$ and α-$NaYF_4$ fluoride single crystals with excellent optical spectra were successfully prepared by using Bridgman method[6,7]. Since fluoride hosts surpass oxide ones in minimum matrix phonon energy and transparency within the infrared wavelength range, it becomes possible to extend the study beyond the limitations of oxide matrices[8,9].

As a fluoride compound, $Na_5Lu_9F_{32}$ possesses good physical-chemical performance and thermal stability. It plays an important role for the doped trivalent rare-earth ions in taking the place of Lu^{3+} ions. On the other hand, its high optical transparency in the infrared range and low phonon energy also make $Na_5Lu_9F_{32}$ single crystal very suitable as potential laser material for the mid-IR laser devices. However, the previous studies about $Na_5Lu_9F_{32}$ doped with rare earth ions were paid more attention on powders and their up-conversions[10]. The $Na_5Lu_9F_{32}$ powders limit their performance because of bad light scattering.

In this paper, the $Na_5Lu_9F_{32}$ single crystal doped with 1% Tm^{3+} (molar concentration) with high optical transparency was grown by Bridgman method. The optical properties of the crystal are investigated from the measured absorption and emission spectra, as well as the decay curve at 1.8 μm under excitation of 790 nm laser diode (LD).

Tm^{3+} doped $Na_5Lu_9F_{32}$ single crystal was grown by an improved Bridgman method. The starting materials were commercially available powders of high purity NaF (99.99%), YF_3 (99.99%), LuF_3 (99.99%) and TmF_3 (99.99%). The molar composition ratio of NaF:LuF_3:TmF_3 is 50:49:1 for $Na_5Lu_9F_{32}$ crystal. These initial compounds were mixed and grounded sufficiently for 1—2 h in a mortar. The mixture was put into apparatus in anhydrous HF atmosphere for fluoridation processing for about 6—8 h at 820 °C to fully remove moisture and impurities in the raw material. The temperature gradient across the solid-liquid interface is 70—90 °C/cm. The crystal growth process was carried out by descending the crucible

* This work has been supported by the National Natural Science Foundation of China (Nos.51472125 and 51272109), the Natural Science Foundation of Zhejiang Province (No.LZ17E020001), and K.C. Wong Magna Fund in Ningbo University.

** E-mail: hpxcm@nbu.edu.cn

with a rate of 0.08 mm/h, which would last about 8—10 days. The detailed description has been described elsewhere[1].

The inserts of Fig.1 show the photos of the high transparent grown crystal with length of 30 mm and diameter of 10 mm and a polished piece. The X-ray diffraction (XRD) of the crystal was recorded by a XD-98X diffraction (XD-3, Beijing). The concentration of Tm^{3+} in $Na_5Lu_9F_{32}$ crystal was measured by an inductively coupled plasma atomic emission spectroscopy (ICP-AES, PerkinElmer Inc, Optima 3000), and the final actual result of the sample is 0.97%. The absorption spectrum was recorded by a Cary 5000 UV/VIS/NIR spectrophotometer over a spectral region from 400 nm to 2 200 nm. The emission spectra were investigated under the excitation of 790 nm LD by a Triax 320 type spectrometer in the range of 1 000—2 200 nm. The fluorescence lifetime was obtained with the FLSP920 fluorescence spectrophotometer. All these properties were measured at room temperature.

In order to identify the chemical phase, the powder XRD pattern of Tm^{3+} doped $Na_5Lu_9F_{32}$ single crystal at the room temperature is shown in Fig.1. By comparing the peak positions with standard JCPDS cards of $Na_5Lu_9F_{32}$ crystal (No.27-0725), the XRD diffraction peaks and relative intensity of the sample are very similar with the standard line patterns. The similar XRD patterns indicate that the sample are crystallized into pure $Na_5Lu_9F_{32}$ crystal, and the doped Tm^{3+} ions don't introduce any obvious peak changes. The bottom section cell parameters can be calculated by

$$d=\frac{a}{\sqrt{h^2+k^2+l^2}}. \tag{1}$$

The cell parameters of $Na_5Lu_9F_{32}$ crystal are calculated to be $a=b=c=0.546\ 6$ nm.

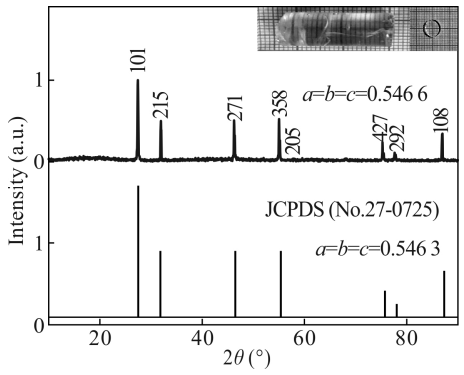

Fig.1 XRD patterns of Tm^{3+} doped $Na_5Lu_9F_{32}$ single crystal and standard JCPDS cards of $Na_5Lu_9F_{32}$ crystal (No.27-0725) (The inserts show the photographs of Tm^{3+} doped $Na_5Lu_9F_{32}$ single crystal and a polished piece.)

Fig.2 illustrates the absorption spectrum of Tm^{3+} doped $Na_5Lu_9F_{32}$ single crystal in the wavelength range of 400—2 200 nm at room temperature. All the bands associate with the energy level diagram of Tm^{3+} ions. It can be seen from Fig.2 that there are six absorption bands of Tm^{3+}, which are located at 461 nm, 653 nm, 678 nm, 770 nm, 1 201 nm and 1 635 nm, corresponding to the transitions from the ground state $^3H_6$ to the excited states $^1G_4$, $^3F_2$, $^3F_3$, $^3H_4$, $^3H_5$ and $^3F_4$ of Tm^{3+} ions, respectively.

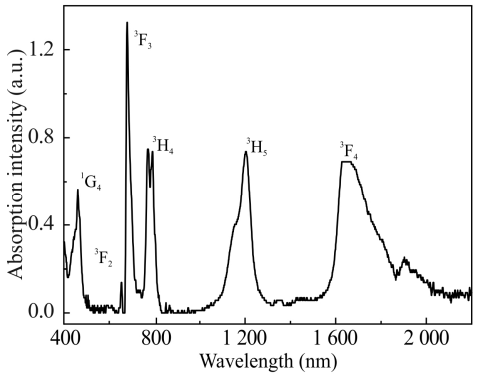

Fig.2 Absorption spectrum of the Tm^{3+} doped $Na_5Lu_9F_{32}$ crystal

Based on the data from above absorption spectrum, the experimental oscillator strengths are obtained by the following expression[11]:

$$f_{\exp}=\frac{mc^2}{\pi Ne^2\lambda^2}\times\frac{2.303}{d}\int OD(\lambda)\mathrm{d}\lambda, \tag{2}$$

where m is the electron mass, e is the electron charge, N is the number of the absorption ions in unit volume, $OD(\lambda)$ is the optical density, c is the speed of light, and d is the thickness of the sample.

According to Judd-Ofelt theory, the calculated oscillator strengths are obtained by

$$f_{\mathrm{cal}}=f_{\mathrm{ed}}+f_{\mathrm{md}}, \tag{3}$$

$$f_{\mathrm{ed}}=\frac{8mc\pi^2}{3h\lambda(2J+1)}\times\frac{(n^2+2)^2}{9n}\times \sum_{t=2,4,6}\Omega_t\left|\left\langle 4f^N[S,L]J\left\|U^{(t)}\right\|4f^N[S',L']J'\right\rangle\right|^2, \tag{4}$$

$$f_{\mathrm{md}}=\frac{h}{6mc\lambda(2J+1)}\times\frac{(n^2+2)^2}{9n}\times \left|\left\langle 4f^N[S,L]J\left\|L+2S\right\|4f^N[S',L']J'\right\rangle\right|^2, \tag{5}$$

where n is the refractive index of samples, λ is the wavelength of the absorption peak, h is the Planck constant, J and J' are the total angular momentum quantum number of the initial and final states, and $\left|\left\langle 4f^N[S,L]J\left\|U^{(t)}\right\|4f^N[S',L']J'\right\rangle\right|$ is the reduced matrix elements.

The root-mean-square (*RMS*) deviation of the experimental and calculated oscillator strengths is defined by

$$\delta=\sqrt{\frac{\sum_{i=0}^{M}(f_{\mathrm{cal}}-f_{\exp})^2}{M-3}}, \tag{6}$$

where M is the number of absorption bands involved in the calculation of the measured line strengths.

Judd-Ofelt parameters Ω_t (t=2, 4, 6) can be calculated

by Judd-Ofelt theory. The experimental and calculated oscillator strengths of Tm^{3+} from the ground state ($^3H_6$) to excited states in the $Na_5Lu_9F_{32}$ crystal and their *RMS* deviation for δ are listed in Tab.1.

Tab.1 The experimental and calculated oscillator strengths of Tm^{3+}:$Na_5Lu_9F_{32}$

Transition	Wavelength (nm)	Oscillator strengths ($\times10^{-6}$)	
		f_{exp}	f_{cal}
$^3H_6\rightarrow{}^3F_4$	1 635	1.608	1.621
$^3H_6\rightarrow{}^3H_5$	1 201	1.414	1.123
$^3H_6\rightarrow{}^3H_4$	770	1.284	1.654
$^3H_6\rightarrow{}^3F_3$	678	1.468	2.281
$^3H_6\rightarrow{}^1G_4$	461	2.342	0.517
δ_{rms} ($\times10^{-7}$)		1.45	

The obtained Judd-Ofelt parameters of Tm^{3+} doped $Na_5Lu_9F_{32}$ crystal compared with those of Tm^{3+} doped other crystals are presented in Tab.2.

Tab.2 Comparison of the Judd-Ofelt parameters for Tm^{3+} doped crystals

Crystals	Ω_2 ($\times10^{-20}$ cm^2)	Ω_4 ($\times10^{-20}$ cm^2)	Ω_6 ($\times10^{-20}$ cm^2)	References
YLF	1.99	1.16	0.69	[12]
LLF	2.12	1.17	1.11	[13]
α-$NaYF_4$	1.31	0.81	0.59	[14]
$Na_5Lu_9F_{32}$	1.02	1.49	0.98	This work

The value of Ω_t is closely related to the matrix structure, the symmetry and the order of the vicinity of rare earth ions in the crystals. According to Judd-Ofelt theory, the symmetry of crystal structure is much higher, and the electrovalent bond is stronger when the value of Ω_2 is much lower. Meanwhile, Ω_2 is sensitive to the environmental configuration symmetry of rare earth ions, and it will decrease with the host material varying from oxide to fluoride. As is shown in Tab.2, the value of Ω_2 in Tm^{3+}:α-$NaYF_4$ single crystal is very similar with that in Tm^{3+}:$Na_5Lu_9F_{32}$ crystal, and both of them are lower than those in Tm^{3+}:YLF and Tm^{3+}:LLF crystals. This comparison confirms that the symmetry of α-$NaYF_4$ and $Na_5Lu_9F_{32}$ crystal structure is much stricter.

Once the intensity parameters are obtained, the electric dipole transition rate A_{ed} from J manifold to lower energy J' manifold can be expressed as

$$A_{ed}=\frac{64\pi^4e^2}{3h\lambda^3(2J+1)}\times\frac{n(n^2+2)^2}{9}\times\sum_{t=2,4,6}\Omega_t\left|\left\langle 4f^N[S,L]J\left\|U^{(t)}\right\|4f^N[S',L']J'\right\rangle\right|^2. \quad (7)$$

The magnetic dipole transition rate A_{md} can be expressed as

$$A_{md}=\frac{64\pi^4e^2}{3h\lambda^3(2J+1)}\times\frac{h^2n^3}{16m^2c^2\pi^2}\times\left|\left\langle 4f^N[S,L]J\left\|L+2S\right\|4f^N[S',L']J'\right\rangle\right|^2. \quad (8)$$

The transition rate A can be deduced by $A(J, J')=A_{ed}+A_{md}$. The fluorescence branching ratio β and the radiative lifetime τ_{rad} can be respectively calculated by:

$$\beta=\frac{A[(S,L)J,(S',L')J']}{\sum_{S'L'J'}A[(S,L)J,(S',L')J']}, \quad (9)$$

$$\tau_{rad}=\frac{1}{\sum_{S'L'J'}A[(S,L)J,(S',L')J']}. \quad (10)$$

All results calculated by above formulas are listed in Tab.3.

Tab.3 The calculated transition rate *A*, luorescence branching ratioβ and radiative lifetime τ_{rad} of Tm^{3+}: $Na_5Lu_9F_{32}$ crystal

J	$\rightarrow J'$	λ (nm)	A_{ed} (s^{-1})	A_{md} (s^{-1})	$\sum A$	β	τ_{rad} (ms)
$^3F_4$	$\rightarrow{}^3H_6$	1 635	93.970		93.970	1.000	10.642
$^3H_5$	$\rightarrow{}^3H_6$	1 201	120.856	44.362	169.827	0.973	5.888
	$\rightarrow{}^3F_4$	3 724	4.490	0.119		0.027	
$^3H_4$	$\rightarrow{}^3H_6$	770	487.048	0.000	549.196	0.887	1.821
	$\rightarrow{}^3F_4$	1 437	31.951	12.039		0.080	
	$\rightarrow{}^3H_5$	2 323	13.816	4.344		0.033	
$^3F_3$	$\rightarrow{}^3H_6$	678	1 211.838	0.000	1 367.677	0.886	0.731
	$\rightarrow{}^3F_4$	1 125	35.994	33.625		0.051	
	$\rightarrow{}^3H_5$	1 612	84.216	0.000		0.062	
	$\rightarrow{}^3H_4$	5 269	1.847	0.157		0.001	
$^3F_2$	$\rightarrow{}^3H_6$	655	368.721	0.000	662.751	0.556	1.509
	$\rightarrow{}^3F_4$	1 059	157.439	0.000		0.238	
	$\rightarrow{}^3H_5$	1 479	132.611	0.000		0.200	
	$\rightarrow{}^3H_4$	4 072	3.971	0.000		0.006	
	$\rightarrow{}^3F_3$	17 920	0.009	0.001		0.000	
$^1G_4$	$\rightarrow{}^3H_6$	461	396.829	0.000	1 016.075	0.391	0.984
	$\rightarrow{}^3F_4$	650	118.268	0.047		0.116	
	$\rightarrow{}^3H_5$	787	296.013	71.802		0.362	
	$\rightarrow{}^3H_4$	1 190	81.024	16.739		0.096	
	$\rightarrow{}^3F_3$	1 537	27.141	0.721		0.027	
	$\rightarrow{}^3F_2$	1 684	7.493	0.000		0.007	

Based on previous absorption spectrum, it can be seen that there is a strong absorption peak at about 800 nm, so 790 nm LD is a very viable pump light source. The emission spectrum for Tm^{3+} doped $Na_5Lu_9F_{32}$ single crystal in the wavelength range of 1 000—2 200 nm excited by 790 nm at room temperature is shown in Fig.3. It can be seen that there are two fluorescence emission

peaks at about 1 480 nm and 1 800 nm, which are respectively corresponded with Tm^{3+} transitions of $^3H_4 \rightarrow {}^3F_4$ and $^3F_4 \rightarrow {}^3H_6$. However, the latter fluorescence intensity is much stronger than that of the former, and the main reason is that the energy spacing between $^3F_4$ and $^3H_6$ is highly close to the energy spacing between $^3F_4$ and $^3H_4$. This can lead to Tm^{3+} at $^3H_4$, which comes from Tm^{3+} at ground state $^3H_6$ transition under the excitation of 790 nm, interacting with Tm^{3+} at ground state $^3H_6$ in the contiguous field. This process is named as cross-relaxation energy transfer process ($2^3F_4 \rightarrow {}^3H_6 + {}^3H_4$), which contributes to the 1.8 μm emission intensity.

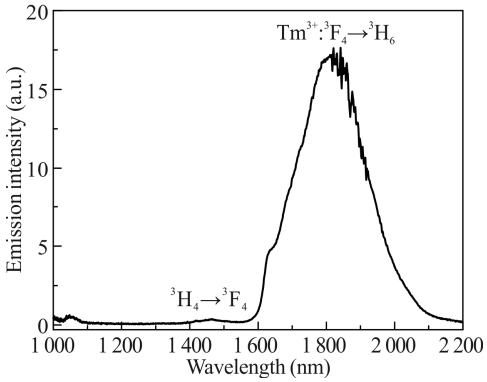

Fig.3 Emission spectrum of the Tm^{3+} doped $Na_5Lu_9F_{32}$ crystal

The absorption cross-section can be measured from the absorption spectrum of Tm^{3+} doped $Na_5Lu_9F_{32}$ single crystal by using following formula:

$$\sigma_{abs}(\lambda) = 2.303 \frac{OD(\lambda)}{Nd} . \tag{11}$$

The stimulated emission cross-section for the laser channel of the $^3F_4 \rightarrow {}^3H_6$ transition can be calculated from the fluorescence spectrum by the McCumber theory:

$$\sigma_{em}(\lambda) = \sigma_{abs}(\lambda) \exp\left(\frac{\varepsilon - hc\lambda^{-1}}{kT}\right), \tag{12}$$

where λ represents the transition wavelength, c is the light velocity, k is the Boltzmann constant (1.38×10^{-23} J/K), h is the Planck constant, T is absolute temperature (here is room temperature), and ε is the free energy needed to excite one Tm^{3+} ion from $^3H_6$ to $^3F_4$ at room temperature (for $^3F_4 \rightarrow {}^3H_6$ transition of Tm^{3+}, $\varepsilon \approx 5\,778$ cm^{-1}).

Observed from cross-section spectrum, the value of emission cross-section at 1 850 nm is about 0.35×10^{-20} cm^2. As one important factor to evaluate the property of a laser, this relatively high value indicates that Tm^{3+} doped $Na_5Lu_9F_{32}$ single crystal can be regarded as a suitable working-laser material.

The calculated stimulated emission cross-section is shown in Fig.4.

Because the fluorescence emission peak located at around 1 850 nm reaches the maximum, the fluorescence decay curve for $^3F_4 \rightarrow {}^3H_6$ transition of Tm^{3+} at 1.8 μm excited by 790 nm LD is measured and shown in Fig.5. At the same time, the comparison of several important parameters among various host crystals is shown in Tab.4.

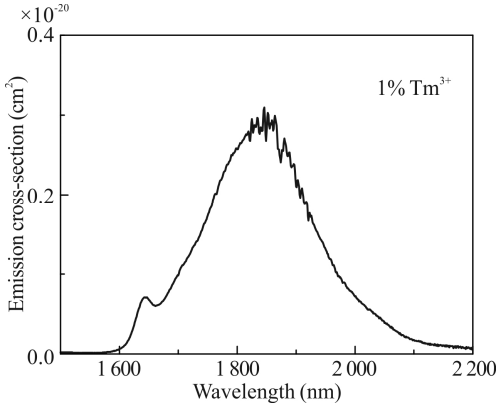

Fig.4 Stimulated emission cross-section of Tm^{3+}:$^3F_4$ manifold

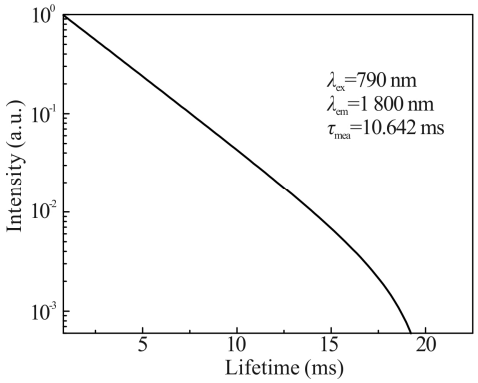

Fig.5 Fluorescence decay curve of Tm^{3+}:$^3F_4$ manifold

Tab.4 Comparison of several important parameters for Tm^{3+} doped crystals

Host crystal	$Na_5Lu_9F_{32}$	α-$NaYF_4$	$LiLuF_4$	$LiYF_4$
Symmetry	Cubic	Cubic	Tetragonal	Tetragonal
Tm^{3+} concentration (%)	1.0	1.0	1.0	1.0
Emission cross-section of $^3F_4$ ($\times10^{-20}$ cm^2)	0.35	0.38	0.3	0.369
Fluorescence lifetime of $^3F_4$ (ms)	10.642	9.937	9.552	8.447
References	This work	[14]	[15]	[15]

From the comparison shown in Tab.4, it is evident that α-$NaYF_4$ and $Na_5Lu_9F_{32}$ crystals exhibit better optical quality, such as fluorescence lifetime and emission cross-section, leading to laser oscillations. But when talks about the contrast between these two Tm^{3+} doped single crystals, it cannot be ignored that there are still some differences between these two samples, although they both have the same cubic system and space group. As for optical properties of Tm^{3+} doped α-$NaYF_4$ single crystal, there has been certainly comprehensive research

in previous work. However, for the study of Tm^{3+} doped $Na_5Lu_9F_{32}$ single crystal, it is still in infancy. Hence, the contradiction in optical parameters is not enough to determine which one is better as a laser hosts between α-$NaYF_4$ and $Na_5Lu_9F_{32}$ crystals. Further theoretical investigations and related experimental works still need to be in progress.

Our experiments demonstrate that Bridgman method is a proper way to grow Tm^{3+} doped $Na_5Lu_9F_{32}$ single crystal. The intensity parameters of Ω_2, Ω_4, and Ω_6 are estimated to be 1.02×10^{-20} cm^2, 1.49×10^{-20} cm^2 and 0.98×10^{-20} cm^2, which are lower than those of Tm^{3+} doped $LiYF_4$ crystal. It meant that the symmetry of $Na_5Lu_9F_{32}$ crystal structure is much stricter. The stimulated emission cross-section at 1.8 μm is calculated to be 0.35×10^{-20} cm^2 for Tm^{3+} doped $Na_5Lu_9F_{32}$ single crystal, which is slightly less than that of Tm^{3+} doped $LiYF_4$ single crystal for 0.369×10^{-20} cm^2. However, the fluorescence lifetime of the Tm^{3+} doped $Na_5Lu_9F_{32}$ single crystal (10.642 ms) is higher than that of Tm^{3+} doped $LiYF_4$ single crystal (8.447 ms). All these spectral properties indicate that the Tm^{3+} doped $Na_5Lu_9F_{32}$ single crystal may be regarded as a potential candidate material for mid-infrared laser application.

References

[1] Wang Cheng, Xia Hai-ping, Feng Zhi-gang, Zhang Zhi-xiong, Jiang Dong-sheng, Zhang Jian, Sheng Qi-guo, Tang Qing-yang, He Shi-nan, Jiang Hao-chuan and Chen Bao-jiu, Optoelectronics Letters **12**, 56 (2016).

[2] Y. F. Li, Y. Qu, Y. M. Sun, X. Y. Hou and H. J. Qi, Acta Photonica Sinica **36**, 591 (2007). (in Chinese)

[3] Pan Cheng, Feng-jing Yang, Zi-zhong Zhou, Bo Huang, Li-bo Wu and Ya-xun Zhou, Optoelectronics Letters **12**, 340 (2016).

[4] Weijie Guo, Yujin Chen, Yanfu Lin, Xinghong Gong,Zundu Luo and Yidong Huang, Journal of Physics D: Applied Physics **41**, 115409 (2008).

[5] N. Coluccelli, G. Galzerano, D. Parisi, M. Tonelli and P. Laporta, Optics Letters **33**, 1951 (2008).

[6] Huiqiong Yan, Xiuqiong Chen, Huangwang Song, Xianghui Wang, Zaifeng Shi and Qiang Lin, Materials Letters **187**, 101 (2017).

[7] Jiang Dong-sheng, Jiang Yong-zhang, Xia Hai-ping, Zhang Jia-zhong, Yang Shuo, Gu Xue-mei, Jiang Hao-chuan and Chen Bao-jiu, Optoelectronics Letters **11**, 356 (2015).

[8] Wu Lei, Zhang Hai-ming, Zhang Jing-Jing, Guo Cong, Ji Zi-ye and Bai Xiao-gang, Journal of Optoelectronics·Laser **26**, 2340 (2015). (in Chinese)

[9] Zheng Jian, Cheng Yin, Wu Zhong-qing, Zhou Wei-wei and Tang Mei-xiang, Journal of Optoelectronics·Laser **26**, 1924 (2015). (in Chinese)

[10] I. M. Shmyt'ko and G. K. Strukova, Physics of the Solid State **51**, 1907 (2009).

[11] Sana J., Cases R. and Alcala R., Journal of Non-Crystalline Solids **93**, 377 (1987).

[12] Wang Peiyuan, Xia Haiping, Peng Jiangtao, Tang Lei and Hu Haoyang, Journal of Optoeletronics·Laser **24**, 2143 (2013). (in Chinese)

[13] Cornacchia F., Palatella L. and Toencelli A., Journal of Physics and Chemistry of Solids **63**, 197 (2002).

[14] Shuo Yang, Haiping Xia, Yongzhang jiang, Jiazhong Zhang, Yiwen Shi, Xuemei Gu, Jianli Zhang, Yuepin Zhang, Haochuan Jiang and Baojiu Chen, Journal of Alloys and Compounds **643**, 1 (2015).

[15] Jing Xiong, Haiyan Peng, Pengchao Hu, Yin Hang and Lianhan Zhang, Journal of Physics D: Applied Physics **43**, 185 (2010).